Adsorption 6, 179–188, 2000

Parametric Study of a Pressure Swing Adsorption Process

W.E. WALDRON AND S. SIRCAR*
Air Products and Chemicals, Inc., 7201 Hamilton Boulevard, Allentown, PA 18195-1501, USA

Received September 2, 1999; Revised February 3, 2000; Accepted February 8, 2000

Abstract. The performance of a pressure swing adsorption (PSA) process for production of high purity hydrogen from a binary methane-hydrogen mixture is simulated using a detailed, adiabatic PSA model. An activated carbon is used for selective adsorption of methane over hydrogen. The effects of various independent process variables (feed gas pressure and composition, purge gas pressure and quantity, configuration of process steps) on the key dependent process variables (hydrogen recovery at high purity, hydrogen production capacity) are evaluated. It is demonstrated that many different combinations of PSA process steps, their operating conditions, and the feed gas conditions can be chosen to produce an identical product gas with different hydrogen recovery and productivity.

Keywords: pressure swing adsorption, methane, hydrogen, process design

Introduction

Separation of bulk gas mixtures by Pressure Swing Adsorption (PSA) processes has become a common industrial practice in the areas of air fractionation, gas drying, and hydrogen production (Sircar, 1996). Numerous PSA process concepts have been patented during the last thirty years and several of them have been commercialized. Besides high separation efficiency and favorable economics provided by some of these processes, the key reason for such a phenomenal growth in the development of this technology is the design flexibility of these processes. Many combinations of the cyclic adsorption, desorption, and complementary steps and their operating conditions in conjunction with a variety of adsorbents (often multiple types used in the same process) can be utilized to obtain the desired separation goals.

Pilot plant performance data are generally needed for ultimate design and optimization of these PSA processes. However, realistic process simulation models can be used for screening process concepts and adsorbent materials, as well as for first pass process design. An acceptable model must simultaneously solve the equations describing the mass, the heat, and the momentum balances in the adsorption columns for each step of the cyclic process and integrate them over many cycles of operation in order to generate the steady state performance. The key input variables for these models include (a) the multicomponent adsorption equilibria, heats, and kinetics for the system of interest covering the entire range of conditions (pressure P, temperature T, and gas phase mole fractions of component i, y_i) experienced by the adsorber during a cycle, (b) the relevant physical properties of the gases and the adsorbents, (c) the fluid dynamic and heat transfer characteristics inside the adsorber, (d) the feed gas conditions, and (e) the sequence of PSA cycle steps, their durations, and operating conditions. The key dependent variables include (a) the product gas purity, pressure, and recovery, (b) the adsorbent inventory needed for producing unit amount of the product, and (c) the specific energy needed for the separation.

It should be emphasized here that the effects of the adsorbent non-isothermality and the column pressure drops on the PSA process steps are critical for obtaining realistic process designs (Hartzog and Sircar, 1995). Ignoring them can result in a very optimistic process

*Author to whom correspondence should be addressed.

performance. Several detailed PSA process models, which incorporate these important effects and which are used for industrial designs, have been published in the literature (Hartzog et al., 1992; Gemmingen, 1993).

The purpose of the present work is to simulate the performance of a PSA process for production of high purity hydrogen from a binary methane-hydrogen feed gas mixture using an adiabatic, non-isobaric model, and to evaluate the effects of feed gas conditions, product purity, and process cycle designs on the separation. It will be demonstrated that the separation performance of the PSA process is the result of a complex and often non-intuitive interaction between the input variables and the process cycle.

Characteristics of the Adsorption System

We chose the BPL activated carbon (Calgon Corp.) for selective adsorption of CH_4 from H_2. Figure 1 shows a set of adsorption isotherms for these pure gases on the carbon at several temperatures over a large pressure range. These data (circles) were experimentally measured in our laboratory using a conventional volumetric adsorption apparatus (Golden and Sircar, 1994). The isotherms can be described very well over the entire ranges of pressure (P) and temperature (T) of the data by the homogeneous Langmuir model (solid lines):

$$n_i^{0^*} = \frac{mb_i P}{1 + b_i P}; \quad b_i = b_i^0 \exp\left[\frac{q_i^0}{RT}\right] \tag{1}$$

where $n_i^{0^*}$ is the specific equilibrium adsorption capacity of pure gas i at P and T. b_i is the Langmuirian

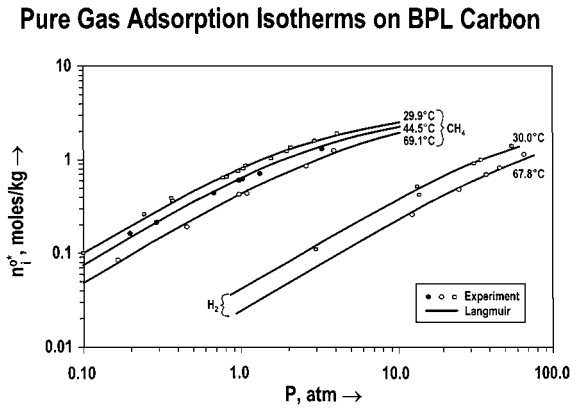

Figure 1. Pure gas adsorption isotherms for CH_4 and H_2 on BPL activated carbon.

Table 1. Equilibrium and kinetic properties of the adsorbent.

	Langmuir equilibrium parameters			Kinetic LDF parameters
Gas	m (moles/kg)	b_i^0 (atm^{-1})	q_i^0 (kcal/mole)	k_i (sec^{-1})
CH_4	3.24	4.32×10^{-4}	3.984	1.3
H_2	3.24	0.87×10^{-4}	3.011	32.5

equilibrium constant for adsorption of pure gas i which is an exponential function of T. b_i^0 is a constant and q_i^0 is the isosteric heat of adsorption of pure gas i which is independent of adsorbate loading and T. m is the saturation adsorption capacity for both gases. Table 1 gives these model parameters. The selectivity (S) of adsorption of CH_4 over H_2 ($S = b_{CH_4}/b_{H_2}$) is a function of T only. The value of S at 30°C is 25.0 and it decreases with increasing T because $q^0_{CH_4} > q^0_{H_2}$.

The mixed gas Langmuir adsorption isotherm is given by

$$n_i^* = \frac{mb_i P y_i}{1 + \sum b_i P y_i} \quad i = 1, 2 \tag{2}$$

where n_i^* is the equilibrium adsorption capacity of component i from a gas mixture (mole fraction y_i) at P and T. It was assumed that the CH_4-H_2 binary adsorption isotherms can be calculated by Eq. (2) using the parameters of Table 1 because our previous experience showed that CO_2-N_2 and CO_2-CH_4 binary mixture data on the BPL carbon can be described by the mixed Langmuir model (Sircar and Kumar, 1986).

Previous analysis of column dynamic data on the BPL carbon for adsorption of CH_4-He, N_2-He, and CO_2-He binary gas mixtures showed that the local adsorption kinetics for these systems can be adequately described by the Linear Driving Force (LDF) model (Sircar and Kumar, 1986):

$$\left(\frac{\delta n_i}{\delta t}\right)_z = k_i[n_i^* - n_i] \tag{3}$$

where k_i is the effective mass transfer coefficient for adsorption of component i. n_i is the instantaneous loading of that component on the carbon at time t and distance z in the column. n_i^* is the corresponding equilibrium loading of component i in the carbon at z and t where the instantaneous gas phase conditions are given by P, T, and y_i.

Table 1 gives the value of k_{CH_4} on the carbon (Sircar and Kumar, 1986). We assumed that hydrogen

Table 2. Physical properties of gases and adsorbent.

Adsorbent

- Bulk density = 0.481 g/cm^3
- Chemical density = 2.107 g/cm^3
- Total column void fraction = 0.77
- Interparticle void fraction = 0.38
- Particle diameter = 3.18 mm
- Adsorbent heat capacity = 0.22 cal/g/°K
- Column diameter = 1.83 m
- Column length = 6.10 m

Gas

- Molar density = Ideal gas
- Molar heat capacity = $C_1 + C_2T + C_3T^2 + C_4T^3$ cal/mole/°K (T = °K)

	CH_4	H_2
C_1	4.75	6.95
C_2	1.20×10^{-2}	-0.046×10^{-2}
C_3	0.303×10^{-5}	0.096×10^{-5}
C_4	-2.63×10^{-9}	-0.208×10^{-9}

- Molar viscosity = $C_1 + C_2T$ kg/m/sec (T = °K)

	CH_4	H_2
C_1	1.75×10^{-6}	2.91×10^{-6}
C_2	3.14×10^{-8}	2.00×10^{-8}

adsorption is instantaneous ($k_{H_2} = 32.5\ \text{sec}^{-1}$). We also assumed that k_i's are independent of n_i and T. These k_i values are relatively large (>1.0 seconds^{-1}) which suggest that the ad(de)sorption process for these systems will primarily be dominated by the adsorption equilibria and the absolute values of these kinetic variables may not be critical (Hartzog and Sircar, 1995).

Table 2 lists the relevant physical properties of the adsorbent and the gas phase used in the simulation. It was assumed that the gas and the adsorbed phases reached instantaneous thermal equilibrium and the adsorbent columns were adiabatic throughout the PSA cycle. It was also assumed that there was no radial gradients and there was no axial dispersions of heat or mass in the column.

It was further assumed that the following differential form of the Ergun equation described the local transient pressure drops in the column at z and t for all steps of the PSA cycle:

$$-\left(\frac{\delta P}{\delta z}\right)_t = \frac{150\mu Q(1-\bar{\varepsilon})^2}{\rho_g (d_p)^2 (\bar{\varepsilon})^3} + \frac{1.75 Q^2 (1-\bar{\varepsilon})}{\rho_g (d_p)(\bar{\varepsilon})^3} \quad (4)$$

where Q is the molar gas flow rate in the column at z and t (based on empty column cross-sectional area). $\bar{\varepsilon}$ is the interparticle void fraction in the column. d_p is the adsorbent particle diameter. μ and ρ_g are, respectively, the gas phase viscosity and density at z and t.

Characteristics of the PSA Process

The base PSA process design for this study consisted of the following seven cyclic steps:

(a) *Adsorption*: The feed gas mixture at pressure P^F and temperature T^F was passed through the carbon column and a stream of pure H_2 at pressure $\sim P^F$ was withdrawn through the product end. A part of this gas was used for final repressurization of a companion column (step g) and the balance was withdrawn as the H_2 product gas. This step was continued until the CH_4 adsorption front reached about the middle of the column.

(b) *Cocurrent Pressure Equalization*: The column was then cocurrently depressurized from P^F to P^I. The effluent gas through the product end consisted of pure H_2 which was used to partially pressurize another column undergoing step (f).

(c) *Cocurrent Depressurization*: The column was then cocurrently depressurized from P^I to P^{II}. The hydrogen effluent gas through the product end was used to purge another column undergoing step (e).

(d) *Countercurrent Depressurization*: The column was then depressurized from P^{II} to P^D countercurrently in order to remove a part of the adsorbed and void gas CH_4 from the column. The effluent gas was wasted.

(e) *Countercurrent Purge*: The column was then purged at the lowest pressure level of the cycle (P^D) countercurrently using a stream of hydrogen from another column undergoing step (c) in order to further remove CH_4 from the column. The effluent gas was wasted.

(f) *Countercurrent Pressure Equalization*: The column pressure was raised from P^D to P^I by countercurrently introducing the effluent gas from step (b) of a companion column.

(g) *Pressurization with Product*: Finally, the column pressure was raised from P^I to P^F by countercurrently introducing a part of the H_2 product gas being produced by another column undergoing step (a). The column was now ready for a new cycle from step (a).

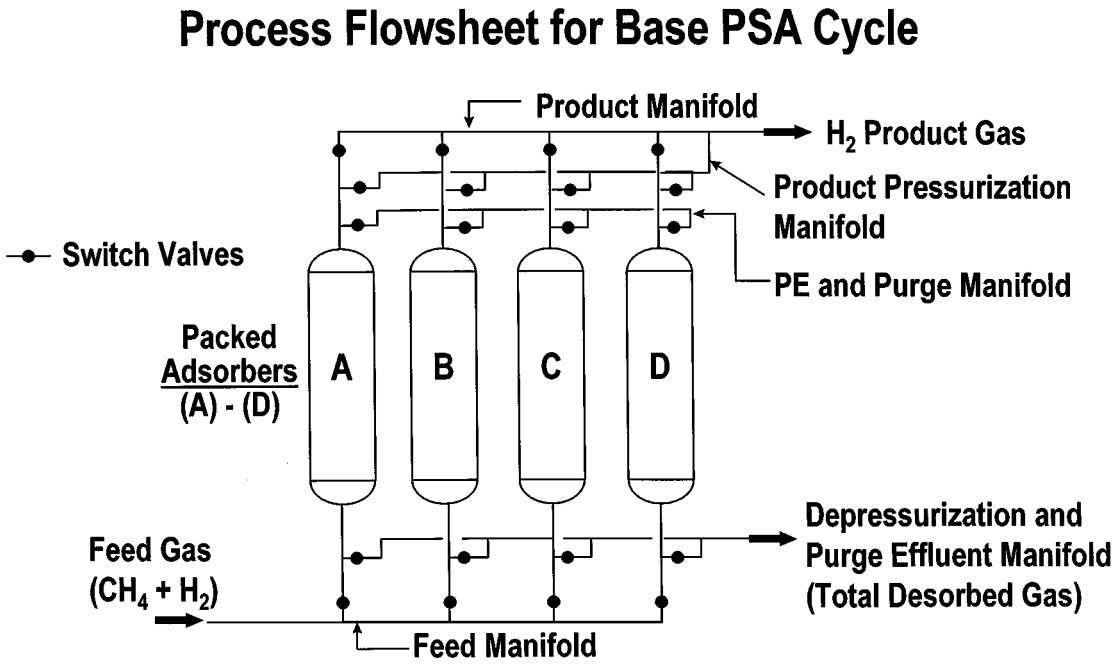

Figure 2. Schematic flow diagram for the base seven-step PSA process.

Figure 2 shows a schematic flow diagram for the above-described PSA process and Table 3(a) gives the time schedule for the steps. Four parallel adsorbers are needed to operate the cycle with continuous feed flow and product gas withdrawal. The only other hardware required by the process are gas headers and switch valves. We assumed that each adsorber was 1.83 meters in diameter and 6.10 meters long, and the total cycle time for the process was 16.0 minutes.

The CH_4 was adsorbed from the feed gas in step (a). It was desorbed and removed from the column in steps (d) and (e). The complementary step (b) is added to recover and internally recycle a part of the void and co-adsorbed H_2 that is present in the column at the end of step (a). The complementary step (c) also recovers a part of the void and co-adsorbed H_2 and uses it as H_2 purge gas during desorption. These steps increase the H_2 recovery by the process at the cost of increased adsorbent inventory. The H_2 purge and pressurization steps (e, f, g), push back the CH_4 impurities from the product end of the column so that a pure H_2 product stream can be obtained during the subsequent adsorption step.

A part of the void gas H_2, the co-adsorbed H_2, as well as the purge gas H_2 is lost with the effluent waste gases produced during steps (d) and (e). This lowers the H_2 recovery by the process. Thus, instead of using one internal pressure equalization (1PE) step (b, f), one may design cycles with two (2PE) or three (3PE) pressure equalization steps in order to improve the H_2 recovery by the process. Table 3(b) and (c) show the cycle steps and time schedules for these cases. For the 2PE case, the adsorber is cocurrently depressurized three times. The H_2 effluents from the first and the third segments are used for pressure equalization with two other companion columns, while the effluent gas from the middle segment is used for the H_2 purge step in another column. This option can be operated using four parallel adsorbers as shown by Table 3(b). For the 3PE case, the adsorber is cocurrently depressurized in four segments. The effluent gases from the first, second, and fourth segments are used for internal pressure equalization with three other companion adsorbers. The effluent gas from the third segment is used to purge another column. It is necessary to have five parallel columns in order to accommodate all the steps of the 3PE case as shown by Table 3(c). It also requires additional valves and piping. The column is countercurrently depressurized to P^D at the end of the cocurrent depressurization steps in all cases, purged with H_2 at P^D, and then repressurized with H_2 to P^F in a sequence of pressure equalization and product pressurization steps.

Table 3. Cyclic steps and various options of times for the PSA process.[a]

(a) One Pressure Equalization Case

Cycle Times (sec)	240	30	60	150	90	150	30	210
Bed A	Adsorption	PE I	Idle	CCD	CoCD	Purge	Pres I/Pres with Product	
Bed B	Pres I/Pres with Product	Adsorption			PE I	Idle	CCD	CoCD	Purge
Bed C	CoCD	Purge	Pres I/Pres with Product		Adsorption			PE I	Idle	CCD
Bed D	PE I	Idle	CCD	CoCD	Purge	Pres I/Pres with Product		Adsorption	

(b) Two Pressure Equalization Case

Cycle Times (sec)	240	30	50	130	30	80	130	30	30	210
Bed A	Adsorption	PE I	Idle	CCD	PE II	CoCD	Purge	Pres I	Pres II/Pres with Product	
Bed B	Pres II/Pres with Product	Adsorption			PE I	Idle	CCD	PE II	CoCD	Purge	Pres I
Bed C	CoCD	Purge	Pres I	Pres II/Pres with Product		Adsorption			PE I	Idle	CCD	PE II
Bed D	PE I	Idle	CCD	PE II	CoCD	Purge	Pres I	Pres II/Pres with Product		Adsorption	

(c) Three Pressure Equalization Case

Cycle Times (sec)	192	30	30	102	30	60	102	30	30	30	132	30	162
Bed A	Adsorption	PE I	PE II	CCD	PE III	CoCD	Purge	Pres I	Idle	Pres II	Idle	Pres III/Pres with Product	
Bed B	Pres III/Pres with Product	Adsorption			PE I	PE II	CCD	PE III	CoCD	Purge	Press I	Idle	Pres II	Idle
Bed C	Idle	Pres II	Idle	Pres III/Pres with Product		Adsorption			PE I	PE II	CCD	PE III	CoCD	Purge	Pres I
Bed D	CoCD	Purge	Pres I	Idle	Pres II	Idle	Pres III/Pres with Product		Adsorption			PE I	PE II	CCD	PE III
Bed E	PE I	PE II	CCD	PE III	CoCD	Purge	Pres I	Idle	Pres II	Idle	EQ1/Prod Repress		Adsorption		

[a]CCD – Cocurrent Depressurization; CoCD – Countercurrent Depressurization; PE – Cocurrent Pressure Equalization; Pres – Pressurization.

The CH_4 impurity is not allowed to break through the product end of the column until at the end of the last cocurrent depressurization steps. Thus, each additional pressure equalization step increases the adsorbent inventory per unit amount of pure H_2 product.

It was assumed in this study that the feed gas was available at pressure P^F and the final desorption pressure (P^D) was slightly above atmospheric. Thus, no additional energy was needed to carry out the separation.

It may be seen from Table 3(a)–(c) that the adsorbers idled during certain periods of the total cycle. There were no introduction or withdrawal of gas from the adsorber during these idle periods. The cycle times for the individual steps were chosen in such a way that the total cycle time was the same for each case and at least one adsorber was always undergoing step (a) of the process so that the feed gas introduction and hydrogen product withdrawal were continuous.

Characteristics of Process Simulation Model

The column mass and heat balance equations used in the model are (Sircar and Rao, 1999):

Component i balance:

$$\left(\frac{\delta \bar{n}_i}{\delta t}\right)_z = -\left[\frac{\delta\{Qy_i\}}{\delta z}\right]_t \quad i = 1, 2 \tag{5}$$

$$\bar{n}_i = \rho_b n_i + \varepsilon \rho_g y_i \quad i = 1, 2 \tag{6}$$

Heat balance:

$$C_s \rho_b \left(\frac{\delta T}{\delta t}\right)_z = -\left[\frac{\delta}{\delta z}\{QC_g(T - T_0)\}\right]_t + \rho_b \sum \left(\frac{\delta n_i}{\delta t}\right)_z + \varepsilon \left(\frac{\delta P}{\delta t}\right)_z \tag{7}$$

where ρ_b, C_s, and ε are, respectively, the adsorbent bulk density, the adsorbent heat capacity, and the total void fraction in the column. n_i, T, and C_g are, respectively, the loadings of component i, the adsorbent and gas temperature, and the molar heat capacity of the gas phase at a distance z in the column at time t. The corresponding gas phase is characterized by P, T, and y_i.

The momentum balance for the column is given by Eq. (4). Equations (4)–(7) can be simultaneously solved with Eqs. (1)–(3) and the appropriate initial and boundary conditions for each step of the PSA cycle to estimate the overall separation performance of the process.

A proprietary software package called SIMPAC (Simulator for Packed Bed Adsorption Cycle) was used. The partial differential equations were discreticized in space using the finite volume method, and the resulting system of time dependent, explicit, first order differential equations was solved with backward difference option for stiff systems. More details about this software package and its operational algorithm can be found elsewhere (Hartzog et al., 1992; Hartzog and Sircar, 1995). About 500 cycles of operation were required before a steady state was reached. On an IBM RS/6000 model 550 workstation with a nominal rating of 25.6 MFLOPS, one complete cycle needed about 68 CPU seconds.

Results of Parametric Study

For our base case analysis, we assumed that the feed gas mixture contained 20% CH_4 + 80% H_2 at a pressure of 14.61 atm (P^F) and a temperature of 30°C (T^F). The countercurrent H_2 purge step was carried out at ~1.34 atm (P^D). The quantity of the H_2 purge gas at the column inlet [P, actual cubic meters (pressure = P^D and temperature = T^F) per cubic meter of carbon column per cycle] during a cycle was controlled by manipulating the rate of the cocurrent depressurization step of the companion column which was producing the purge gas. The H_2 product gas purity was 99.999% in all cases except otherwise mentioned. The separation performance of the process was estimated in terms of the H_2 productivity [H, normal cubic meters (pressure = 1 atm and temperature = 21°C) per cubic meter of carbon column per cycle] and the % H_2 recovery [R, moles of H_2 produced per mole of H_2 feed per cycle × 100]. The preferred performance objective was to increase both H and R while maintaining the product gas purity.

Effect of PSA Cycle Design

We conducted a series of simulation runs for the process options 1PE, 2PE, and 3PE using different H_2 purge gas quantities (P). Feed gas quantities [F, actual cubic meters (pressure = P^F and temperature = T^F) per cubic meter of carbon per cycle] were adjusted to meet the desired product purity. The model generated the composition-quantity profiles for the effluent gases from the countercurrent depressurization and the countercurrent H_2 purge steps. They were integrated to obtain the amount of H_2 lost by the process per cycle. Consequently, the H_2 recovery by the process was estimated.

Figure 3 shows typical CH_4 desorption characteristics by the process. It was generated for a 1PE cycle using a P/F value of ~1.0. The abscissa for Fig. 3 represents the fraction (f) of the total gas leaving the column during steps (d) or (e). It may be seen from Fig. 3 that $y^D_{CH_4}$ increases as the desorption process by countercurrent pressure reduction continues and $y^P_{CH_4}$ decreases as the desorption process by hydrogen purge continues. The figure also gives the average column pressures during these two steps. The fraction of H_2 loss during the pressure reduction step is 38.6% of the total H_2 loss for this case.

Figure 4 summarizes the net results of these runs which show the hydrogen productivity (H) and the recovery (R) as functions of P/F for all three different process cycle options. The general trend is that both H and R are relatively low when P/F is low. They both increase with increasing P/F, go through maximum

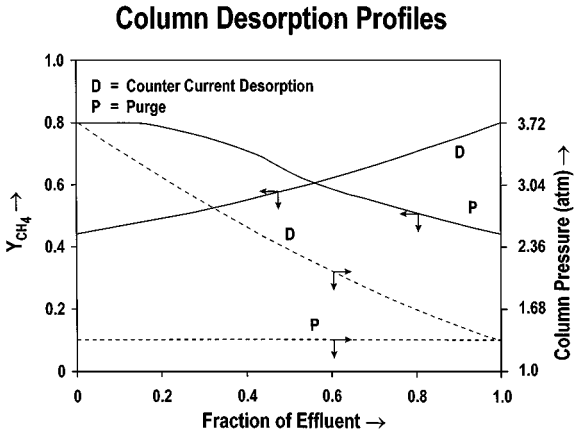

Figure 3. Example of effluent gas composition—quantity profiles for countercurrent depressurization and hydrogen purge steps of the base PSA process.

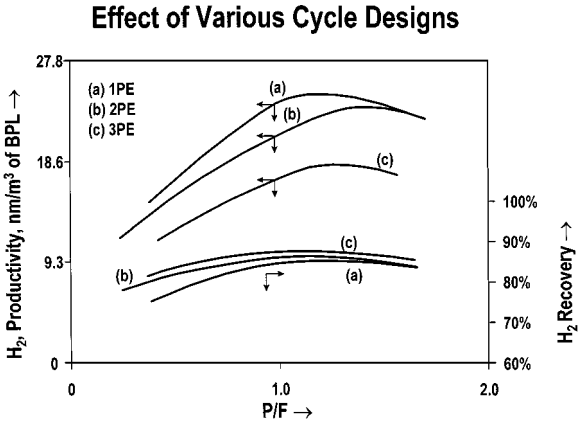

Figure 4. PSA process performance using one-, two-, and three internal pressure equalization steps.

values, and then decrease as P/F is further increased. At lower P/F ratios, a relatively larger fraction of adsorbed CH_4 is desorbed per unit amount of H_2 purge used in the process. Thus, both the H_2 productivity and recovery increase with increasing P/F. At higher P/F ratios, the amount of desorbed CH_4 per unit amount of purge gas used decreases, which reduces both the H_2 productivity and recovery values. The variation of R is much less pronounced than that for H. It may be interesting to note that the maximum of H and R profiles do not occur at the same value of P/F. Thus, both advantages cannot be achieved at the same time. Higher H_2 recovery may, however, be economically more attractive than higher H_2 productivity.

The data of Fig. 4 also shows that for any given value of P/F, higher H_2 recovery can be achieved by increasing the number of pressure equalization steps. The H_2 productivity, on the other hand, drastically decreases in the order 1PE > 2PE > 3PE. The maximum values of H_2 recoveries for these three cases are, respectively, 85.0%, 86.5%, and 87.5%. The H values for these maximum H_2 recovery levels are, respectively, 24.7, 22.1, and 17.7. Thus, a 2.5 point additional H_2 recovery (%) can be obtained over 1PE case by using the 3PE cycle at the cost of ∼40% more adsorbent inventory for the same H_2 production rate. The optimum values of P/F for the highest R values for all three cases lie between 1.1–1.3. The 3PE case also requires additional hardware to accommodate five adsorbers in the process.

Table 4. Hydrogen losses during countercurrent depressurization and purge[a].

Process cycle	H_2 loss in countercurrent depressurization H_2 in feed	H_2 loss in purge effluent H_2 in feed
1 Equalization	0.058	0.092
2 Equalizations	0.024	0.117
3 Equalizations	0.010	0.118

[a] All absolute quantities are in moles of gas/kg of adsorbent/cycle.

Table 4 shows the amounts of H_2 lost during the countercurrent depressurization and H_2 purge steps of the PSA process using the 1PE, 2PE, and 3PE options when the H_2 recoveries are at their maximum values. The amount of fractional H_2 loss during the countercurrent depressurization step decreases as the number of internal pressure equalization steps are increased. The fractional H_2 loss during the countercurrent H_2 purge step does not significantly change between these process options.

Effect of Feed Gas Pressure

Figure 5 shows the performance of the PSA process with a one (1PE) or three (3PE) pressure equalization steps, estimated using different feed gas pressures. The P/F ratio was maintained at a constant value of ∼1.0 for these runs. In both cases, the H_2 productivity monotonically increased as the feed gas pressure is increased but the H_2 recovery went through a maximum value. The higher feed gas pressure results in higher void and co-adsorbed H_2 in the column at the start of the step (d) which is then lost during countercurrent desorption, causing a larger reduction in H_2 recovery by the process.

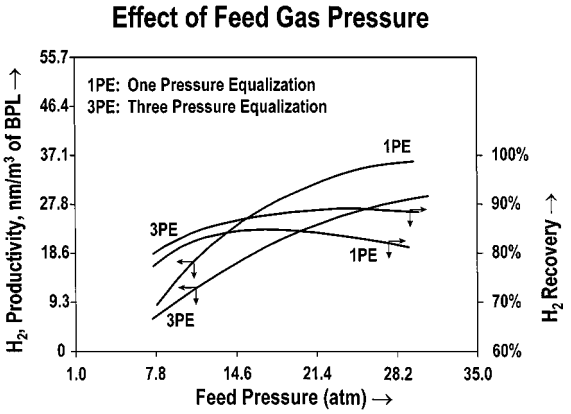

Figure 5. PSA process performance using different feed gas pressures and pressure equalizations steps.

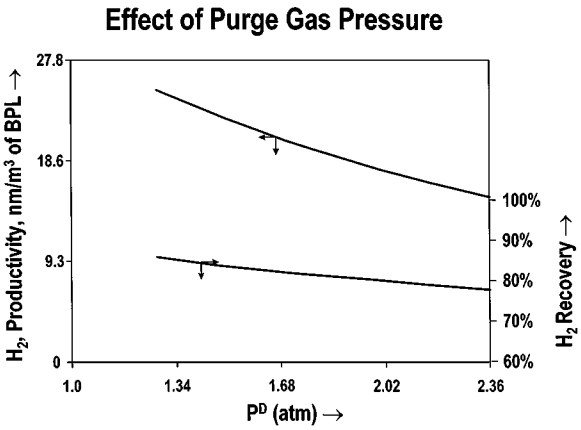

Figure 6. Effect of hydrogen purge gas pressure on the performance of the PSA process.

Figure 5, however, shows some very interesting results. Both the H_2 recovery and the productivity are comparable between the 1PE and 3PE cases when the feed gas pressure is relatively low ($P^F \sim 7.80$ atm). Thus, there is no incentive to use the 3PE cycle in that pressure range. The H_2 recovery, on the other hand, is much higher for the 3PE option than the 1PE case in the higher feed pressure range. Thus, the 3PE case is much superior in that region. The maximum in the H_2 recovery-pressure profiles occurs at a much lower feed pressure value for the 1PE case than for the 3PE case.

Figure 5 also shows that the H_2 recovery is higher for the 3PE case than the 1PE case but the corresponding H_2 productivity is lower. The two extra cocurrent pressure equalization steps in the 3PE case decrease the subsequent H_2 loss in the countercurrent depressurization step which increases the H_2 recovery by the process. On the other hand, these steps require more adsorbent volume to contain the CH_4 impurities from breaking through which reduces the H_2 productivity.

Effect of Purge Gas Pressure

The purge gas pressure (P^D) is a key variable in the PSA process because the purge waste gas is often piped for combustion. Figure 6 shows the performance of the base PSA process with one pressure equalization step and using different purge gas pressures. Both H and R drastically decreased as the purge gas H_2 pressure was increased. Lower purge gas pressure was obviously beneficial.

Effect of H_2 Product Purity

The base PSA process (1PE case) can be operated to produce lower purity H_2 by allowing some of the CH_4 impurity to break through during the last cocurrent depressurization step. Table 5 shows the H and R values for several levels of CH_4 impurities in the product gas. The H_2 productivity and recovery increased as the H_2 purity in the product gas was reduced. Alternatively, the table shows that the penalty for increasing the product H_2 purity from 99.0–99.999% was not large. Only a 14% reduction in H_2 productivity and a 2.5 points decrease in H_2 recovery occurred during such a large upgrade in the H_2 product purity. This is a typical advantage offered by most PSA processes which cannot be met by many other separation technologies.

Effect of Feed Gas Composition

Several simulation runs were also made using different feed gas compositions (60–90% H_2) and the base PSA

Table 5. Performance of the PSA process for producing impure hydrogen product.

Product H_2 purity (mole %)	H_2 productivity (H) (nm^3/ft^3)	H_2 recovery (R) (%)	P/F
99.999	24.21	84.8	1.01
99.990	25.03	85.5	0.98
99.900	26.16	86.3	0.94
99.000	27.62	87.4	0.93

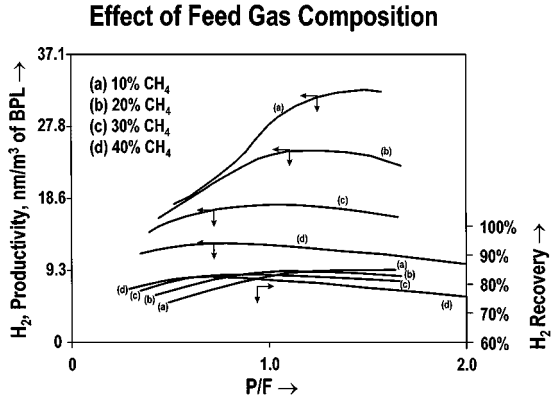

Figure 7. PSA process performance using different feed gas compositions.

process with a single pressure equalization step. The H_2 product purities were again maintained at 99.999% for these cases. Figure 7 shows the results which plot H and R values as functions of P/F for feed gas mole fractions ($y^F_{H_2}$) of 60%, 70%, 80%, and 90% H_2. The general characteristics of these curves are similar to those shown by Fig. 4. Again the maximum values of H and R for any given value of $y^F_{H_2}$ did not occur at the same value of P/F.

A very interesting result was that the maximum values of H_2 recovery changed only between 82.5–85.5% when $y^F_{H_2}$ was changed from 60–90%. The higher the feed gas H_2 mole fraction, the higher was the maximum value of the H_2 recovery. On the other hand, the corresponding change in the maximum values of H_2 productivity was very large. The maximum H_2 productivity values were, respectively, 32.1, 24.5, 17.6, and 12.8 for $y^F_{H_2}$ values of 90%, 80%, 70%, and 60%. Thus, higher H_2 concentration in the feed gas does not appreciably increase the potential H_2 recovery but it significantly increases the H_2 productivity (reduces adsorbent inventory). As in the case of Fig. 4, the effect of varying P/F on H_2 recovery is much less pronounced than that on H_2 productivity.

This parametric study demonstrates the flexibility in the design and operation of a PSA process for CH_4-H_2 separation. Various combinations of process steps, operating conditions, and feed gas conditions can be used to produce the same product purity with different H_2 recovery and productivity. Some of the results of this study are not obvious. They are caused by complex interactions between the adsorptive properties of the system and the process design. This may complicate the process optimization, but it also creates opportunities for developing new PSA process concepts.

Summary

Separation of binary methane-hydrogen gas mixture by a PSA process using one or more internal pressure equalization steps was numerically evaluated. An activated carbon, which selectively adsorbed methane over hydrogen was used as the adsorbent. An adiabatic, nonisobaric PSA model called SIMPAC was employed for the process simulations. The effects of different process designs, the feed gas pressure and composition, the product H_2 purity, and the hydrogen purge gas pressure on the process performance were evaluated. Hydrogen recovery and hydrogen productivity per unit amount of the adsorbent were treated as the dependent variables.

The key conclusions reached from this study are:

(a) High purity H_2 product (99.999 mole%) can be produced at feed gas pressure from a feed gas mixture containing 60–90 mole% H_2.
(b) Both the H_2 recovery and productivity exhibit maximum values as functions of the actual H_2 purge to feed gas volumes per cycle. However, the locations of these two maximum properties do not coincide. Thus, one cannot take advantage of both features.
(c) The H_2 recovery can be increased by increasing the number of internal pressure equalization steps (PE) in the PSA cycle at the cost of a significant reduction in the H_2 productivity.
(d) The H_2 productivity of the PSA process monotonically increases when the feed gas pressure is increased but the H_2 recovery-feed gas pressure profile goes through a maximum value at high pressures. There is minimal incentive to use the 2PE or 3PE case over the 1PE case when the feed gas pressure is relatively low ($P^F \sim 7.80$ atm). The hydrogen recovery is much higher for the 3PE case at higher feed gas pressures.
(e) Increasing the hydrogen purge gas pressure drastically decreases both the hydrogen recovery and the productivity.
(f) The H_2 product purity can be upgraded from 99.0% to 99.999 mole% with a relatively small penalty in hydrogen recovery and productivity.
(g) The maximum hydrogen recovery is a relatively weak function of the feed gas composition (60–90 mole% H_2 range) but the H_2 productivity increases

significantly when the hydrogen mole fraction in the feed gas is increased.

(h) Many different combinations of PSA process steps, their operating conditions, and the feed gas conditions can be chosen to produce an identical product gas with different hydrogen recovery and productivity. This complicates the task of process optimization, but it also creates newer opportunities.

References

Gemmingen, U.V., "Pressure Swing Adsorption Process—Design and Simulation," in *Proceedings of 4th Int. Conf. on Fundamentals of Adsorption*, Kyoto, Kodansha, Japan, 1993, M. Suzuki (Ed.), pp. 703–712.

Golden, T.C. and S. Sircar, "Gas Adsorption on Silicalite," *J. Colloid and Interface Sci*., **162**, 182 (1994).

Hartzog, D.G., V.G. Fox, R. Kumar, Y.C. Chen, P.A. Houghton, and T. Naheiri, "A Versatile Process Simulator in Adsorptive Separations," in *Paper Presented at AIChE Meeting*, Miami, Florida, 1992.

Hartzog, D.G. and S. Sircar, "Sensitivity of PSA Process Performance to Input Variables," *Adsorption*, **1**, 133 (1995).

Sircar, S., "Adsorption," in *The Engineering Handbook*, R.C. Dorf (Ed.), Ch. 59, pp. 604–617, (1996). CRC Press, Boca Raton, Florida.

Sircar, S. and R. Kumar, "Column Dynamics for Adsorption of Bulk Gas Mixtures on Activated Carbon," *Sep. Sci. Tech.*, **21**, 919 (1986).

Sircar, S. and M.B. Rao, "Heat of Adsorption of Pure Gas and Multicomponent Gas Mixtures on Microporous Adsorbents," in *Surfaces of Nanoparticles and Porous Materials*, J.A. Schwarz and C.I. Contescu (Eds.), Ch. 19, pp. 501–528, Marcel and Dekker, New York, 1999.